

An expanded model for predicting surface coal mine drill respirable dust emissions

Steven J. Page*, Randy Reed and Jeffrey M. Listak

Department of Health and Human Services, Centers for Disease Control and Prevention, National Institute for Occupational Safety and Health, Pittsburgh Research Laboratory, Pittsburgh, PA, USA

(Received 25 October 2007; accepted 19 November 2007)

Overexposure to airborne respirable crystalline silica dust can cause disabling or fatal respiratory disease, and mine worker exposure to silica dust continues to be an ongoing occupational health concern. Exposures of surface coal mine rock drillers to respirable crystalline silica are of particular concern. On surface coal mine drills, bailing air flushes the cuttings out of the drill hole. Conveyor belting material is typically used to fabricate a shroud around the drill deck in an effort to contain the drill dust so that it can be captured by a collector. Dust leakage from the drill shroud is usually the worst dust source problem on most drills. The focus of this work is drill shroud dust leakage and the relationships of various drill parameters on this leakage. Experimental data were obtained and used in combination with dimensional analysis to establish these relationships. In general, it is found that airborne respirable dust (ARD) concentrations vary in a direct relationship with shroud leakage area and in an inverse relationship with drill deck cross-sectional area and shroud height. This work expands the testing and dimensional analysis previously reported for collector/bailing air flow ratios ranging from 2:1 to 4:1 to include ratios approaching 1:1. A semi-empirical mathematical model has been developed and expanded to describe ARD generation on surface coal mine drills. Geometric parameters included are drill deck height and cross-sectional area, shroud leakage associated with the deck shroud, and the operational parameters of bailing airflow and dust collector airflow. The relationships can be described by logarithmic functions and yield predictive ARD values, which fall in the range measured on operating drills for collector/bailing air flow ratios greater than 2. However, at values of collector/bailing air flow ratios of approximately 1.1, the amount of ARD shows minimal response, if any, to drill deck shroud improvements that do not result in near-perfect seals. This is a condition that can occur in actual operation and is a substantially different result than previously expected and reported. Application of these results should provide mine operators with sufficient information to determine (1) the relative magnitude of their dust emissions, (2) where they should focus their efforts to reduce ARD emissions and (3) the improvement they could reasonably expect to achieve. Given that exposures of surface coal mine rock drillers to respirable crystalline silica are of particular concern, substantial reductions of airborne silica dust during drilling may be estimated and achieved through use of the analysis presented.

Keywords: drill; dust; model; dimensional analysis

*Corresponding author. Email: sep8@cdc.gov

1. Introduction

Overexposure to airborne respirable crystalline silica dust can cause serious or fatal respiratory disease. Exposures of surface coal mine rock drillers to respirable crystalline silica are of particular concern. In a 1992 Alert on silicosis in rock drillers, the US National Institute for Occupational Safety and Health (NIOSH) reported on 23 cases of advanced silicosis (acute, accelerated and chronic) in workers ranging in ages from 25 to 60 with drilling tenures ranging between 3 and 20 years [1]. Most of the cases involved drill operators in their 30s and 40s, indicating that high silica exposure levels are associated with their occupation. A more recent lung X-ray surveillance study of a 664 volunteer population of surface coal miners showed that the prevalence of silicosis-like abnormalities was 9% [2]. The two most significant factors associated with these silicosis-like abnormalities were increasing age and years of drilling experience.

The US Mine Safety and Health Administration (MSHA) permissible dust exposure for coal mine workers is an 8 h shift average of 2.0 mg m^{-3} of airborne respirable coal mine dust, as defined by the Mining Research Establishment (MRE) Criteria [3]. If the airborne respirable dust (ARD) sample contains more than 5% crystalline silica, the dust standard is reduced to the quotient of 10 divided by the percentage of silica in the dust, limiting the respirable crystalline silica exposure to a maximum of $100 \mu\text{g m}^{-3}$ (MRE equivalent) for the working shift. Compliance with these respirable dust standards is expected to significantly reduce a worker's risk of occupational lung disease throughout an average life expectancy.

MSHA dust exposure data from 1985 to 1992 (operator and MSHA inspector-collected samples) showed that the percentage of the designated work position (DWP) highwall drill dust samples having greater than 5% silica and exceeding the $100 \mu\text{g m}^{-3}$ silica limit were 81% and 77%, respectively [4]. A special MSHA inspector sampling survey of non-designated work positions (NDWP) at surface coal mines showed very similar silica dust level results for the highwall drill operator as compared to the DWP sampling data. NDWP work positions are not designated for routine sampling by coal mine operators and are only sampled by MSHA inspectors. DWPs are work positions that MSHA has designated for operator sampling. The percentage of NDWP highwall drill operator samples having greater than 5% silica content and exceeding the $100 \mu\text{g m}^{-3}$ silica limit were 81% and 75%, respectively [4]. Although, a recent analysis of the MSHA data from 2000 to 2006 shows that the percentage of the DWP drill dust samples exceeding the permissible exposure limit has dropped to 16%, MSHA data still suggests that overexposure to silica dust is an ongoing surface coal mine dust problem for the highwall drill operator. The 1992 Alert enabled MSHA to promulgate new dust regulations in 1994 requiring mine operators to provide effective drill dust control, regardless of exposure. These regulations permitted MSHA to cite a mine operator when a dust control is missing, not maintained, defective or ineffective, generally based on a visual inspection. Enforcement of this regulation led to the significant decline in the number of samples exceeding the standard.

On surface coal mine drills, bailing air flow flushes the cuttings from the hole. The material is ejected from the hole at ground level with significant velocity. In an attempt to control/capture the respirable dust emitted from the hole, a deck shroud encloses the area around the drill deck and an external dust collector is used with its duct inlet typically located in the upper outboard rear corner of the enclosed deck volume. Frequently, the deck shroud is made merely by hanging four pieces of rubber belting from the deck. This obviously leaves gaps at the corner seams for dust to escape. Additionally, the shroud does

not always reach the ground, leaving a gap around the bottom perimeter of the shroud where dust can escape. Dust leakage from the drill shroud was observed to be one of the worst dust emission problems on many drills. However, other dust generation sources were also present on these drills besides the shroud leakage. These include dust escaping through the drill stem seal at the top of the drilling table; dust entrained from the dumping of collector fines on the mine bench; and dust discharged out the collector's exhaust because of impaired filter capture [5].

The focus of this present work is drill shroud dust leakage and the relationships of various drilling parameters on this leakage at low dust collector airflows. Experimental data were obtained on an improved full-scale test facility and used in combination with dimensional analysis to establish these relationships. This work expands the testing and dimensional analysis previously reported [6] for collector/bailing air flow ratios ranging from 2:1 to 4:1 to include ratios approaching 1:1, a condition that can occur in actual operation. A significantly different result than previously expected and reported was obtained for airflow ratios below 2:1.

2. Experimental methods

2.1. Test facility

Testing was performed on a full-scale mockup, as previously reported with a detailed diagram of the test facility [6], of a drill deck and shroud, including drill pipe and drill hole, enclosed within a large chamber. The following are brief descriptions of each component and the improvements made since the previous publication.

The drill deck and shroud were constructed of plywood and stud framing with final dimensions measuring 1.22 m (4 ft) wide by 1.52 m (5 ft) long by 1.22 m (4 ft) high. Each plywood side panel of the shroud was constructed in hinged segments so that shroud leakage areas A_L corresponding to shroud-to-ground gaps (h) of 51 mm (2 in.), 203 mm (8 in.) and 356 mm (14 in.) could be readily simulated.

The drill pipe and drill hole were simulated by a 152 mm (6 in.) schedule 40 pipe concentrically mounted inside a 203 mm (8 in.) schedule 80 pipe, respectively. The larger outside pipe bottom was capped off to simulate the hole bottom and the inside pipe was suspended in a fixed position to provide adequate clearance between the two pipe ends to accommodate the bailing air flow rate. The complete pipe assembly extended approximately 0.61 m (2 ft) above the drill deck and 0.91 m (3 ft) below the floor of the large test chamber (to be described shortly).

One of the most significant improvements made to the test facility was the installation of a state-of-the-art air compressor to deliver the bailing air volumetric flow rate Q_B . A Kaeser DSD125 compressor capable of delivering $19.5 \text{ m}^3 \text{ min}^{-1}$ @ 758 kPa (690 cfm @ 110 psi) was equipped with an oil separator as well as a refrigeration unit for significant water removal and the maintenance of a low and constant air temperature. Bailing air was supplied to the top of the inside pipe in two separate splits. The main split of air was regulated between 13.6 and $14.1 \text{ m}^3 \text{ min}^{-1}$ (482 and $499 \text{ ft}^3 \text{ min}^{-1}$) after bailing air temperature and pressure correction. The corrections were required to compensate for deviations from the conditions at which the flow meter was calibrated. The main split temperature and pressure for all the tests varied from 288 to 297 K (59–75°F) and 200 to 214 kPa (29–31 psi), respectively. The secondary split of air was regulated between 0.71 and $0.76 \text{ m}^3 \text{ min}^{-1}$ (25 and $27 \text{ ft}^3 \text{ min}^{-1}$) after bailing air temperature and pressure correction. The secondary split temperature and pressure for all the tests varied from 290 to 298 K (63–76°F) and

331 to 345 kPa (48–50 psi), respectively. Therefore, the total bailing air flow rate varied between 14.4 and 14.9 m³ min⁻¹ (508 and 525 ft³ min⁻¹). This total volumetric airflow was approximately 4.3 m³ min⁻¹ (150 ft³ min⁻¹) greater than in tests previously reported. The secondary air split was used to drive a venturi eductor. This eductor and secondary air split injected the test dust into the side of the drill pipe near the top to be mixed with the main split of air.

A dust collector was used to provide exhaust ventilation volumetric flow rate Q_C within the deck shroud via ductwork connected to the top of the drill deck in one corner. This configuration is typical on nearly all rotary drills equipped with a dry dust collector. Four different collector air flows were evaluated as one of the test parameters and were obtained by regulation of a bleed air inlet at the collector. A broad range of parameters was chosen based on parameters typically found on operating rotary drills. However, the ratio $Q_C/Q_B = 3.0$ is usually the maximum design value found on drills with clean collector filters. The ratio $Q_C/Q_B = 2.0$ is typically a much more common value found in actual operation for dust collectors with loaded filters that should be replaced. The ratio $Q_C/Q_B = 4.0$ was also chosen for testing to ensure that the region of maximum curvature in the dependent variable was included in the testing protocol, as well as to evaluate the effect of increasing the dust collector air flow on ARD concentrations. The ratio $Q_C/Q_B = 1.1$ was a new test condition to examine if the functional relationships for the other airflow ratios are still applicable since this condition has been observed in actual drill operations. Values of $Q_C/Q_B \leq 1$, although possible in practice, would represent a condition with airborne dust escaping the test chamber.

To provide a suitable dust sampling environment, the drill deck, drill pipe and shroud were located within a larger chamber measuring 3.05 m (10 ft) wide by 3.66 m (12 ft) long by 2.44 m (8 ft) high and elevated 0.91 m (3 ft) above ground level. The top of the chamber was equipped with three adjustable louvers to provide makeup air to allow for the difference between the bailing airflow into the chamber and the dust collector airflow out of the chamber. The louvers were adjusted according to the airflow requirements so that the air velocity in each louver was approximately constant at 1.02 m s⁻¹ (200 ft min⁻¹) to keep dust from escaping out of the chamber. The chamber dimensions were chosen based on two requirements: (1) to allow ample room around the drill deck shroud, and (2) to maintain an average makeup air velocity within the chamber of no more than 3.24 m min⁻¹ (11 ft min⁻¹) to minimise the effect on the dust escaping the shroud.

2.2. Dust generation and test procedures

The commercially available limestone test dust (100% < 74 µm or 200-mesh) was fed into the eductor by a Vibra-Screw feeder. Limestone was chosen as a surrogate test dust because it is much safer to use than silica and has virtually the same density. In reality, choice of test dust is not critical because dust sampling is performed on an aerodynamic size classification basis. A change to a smaller auger feed screw in the feeder was the second improvement in the test facility. This change was made to help improve the uniformity of the dust feed rate by reducing the void space within the auger as well as allowing for a faster auger rotation. The auger feed rate was adjusted by a motor controller to produce an approximately constant feed rate, timed for a 3-min interval. A tachometer motor voltage output was used to monitor the feed rate during the test. The feed rate was measured before and after each test, and the two values were averaged to

estimate the feed rate during the test. The feed rate for all tests averaged $4727 (\pm 482)$ mg min^{-1} .

The collector airflow velocity pressure for each test was set prior to each test and recorded for a 5-min interval before and after the test with a pitot tube. The pitot tube was removed prior to feeding dust into the chamber and during the test. Static pressure in the collector duct, relative to the inside of the test chamber, was monitored and continuously recorded for the entire test duration.

Gravimetric samplers using 37 mm filter cassettes and 10 mm Dorr-Oliver cyclones were used to measure respirable dust levels inside the chamber. The tests were randomised and followed a two-level factorial design with two centre points using the variables of collector airflow and leakage area, maintaining constant bailing airflow. Two samplers were used on each of the four sides of the shroud and located approximately 0.61 m (2 ft) above the floor level. Previous testing relied on individual air sampling pumps typically used with the cyclones. This required periodic calibration as well as turning all pumps on/off at slightly differing times.

The next significant change in the test facility was the method used to regulate sampler air flow rates. The sampling pumps were replaced with critical orifices and one vacuum pump to maintain constant flow rate. Consequently, all samplers were turned on/off simultaneously. The samplers were operated at a flow rate of 2.0 L min^{-1} . A RAM-1 instantaneous dust monitor was used at one location within the chamber to monitor the dust concentration during the pre-test dust feed and during the test. The analog output of the RAM-1 was fed to a strip chart recorder for visual monitoring of the dust concentration stability. Dust sampling time was fixed at 50 min after verification that the chamber dust concentration had stabilised. The final chamber dust concentration was determined from the average of the eight gravimetric samples.

3. Theoretical analysis

The concept of dimensionless parameters, based on variables which are known to be the most influential, permits a limited amount of experimental data to be applied to other configurations of geometry, forces, air flows, velocities, etc. However, a detailed derivation of the dimensional analysis technique known as the Buckingham Π theorem [7] shall not be presented in this work. Also, development of the theoretical analysis pertaining to this work has been previously published [6] and will not be presented in this work.

The following variables are known from experience to be the most influential in terms of drill ARD generation and are defined in this study as:

R = dust feed rate (gm min^{-1})

C = ARD concentration emanating from shroud leakage, mg m^{-3} , the dependent variable in the analysis

Q_B = bailing air flow ($\text{m}^3 \text{min}^{-1}$)

Q_C = collector air flow ($\text{m}^3 \text{min}^{-1}$)

h = open shroud-to-ground gap height (m)

H_S = shroud height (m)

H_{Sc} = effective shroud height (m), determined by the experimental shroud height H_S minus the leakage height h

A_S = cross-sectional area of drill deck shroud (m^2)

A_L = leakage area of deck shroud (m^2)

Reiterating, it is assumed that the leakage area A_L is restricted to the bottom gap area and that no leakage occurs at the vertical corners of the deck shroud. Published reports demonstrate that this condition can be achieved in practice [8,9]. The convention used for the analysis and presentation of data will assume that H_S is the respective effective height H_{Se} . From dimensional analysis [6], the Π parameters are determined to be

$$\Pi_1 = Q_C C/R, \quad \Pi_2 = Q_B/Q_C, \quad \Pi_3 = H_S/A_L^{0.5}, \quad \text{and} \quad \Pi_4 = A_S/A_L \quad (1)$$

The grouped data in Table 1 can be presented in the form [6]

$$\Pi_2 * \Pi_1 = a \ln(\Pi_3) + b \quad (2)$$

Table 1. Shroud test data.

Test	Q_C/Q_B Target	Q_C ($\text{m}^3 \text{min}^{-1}$)	Q_B (m^3 min^{-1})	Q_C/Q_B Actual	h (m)	H_{Se} (m)	A_L (m^2)	R (gm min^{-1})	ARD (mg m^{-3})
NB-1	1.1	16.4	14.6	1.13	0.051	1.168	0.24	4.7	13.01
NB-15	1.1	16.6	14.7	1.13	0.051	1.168	0.24	5.2	10.39
NB-18	1.1	16.5	14.8	1.11	0.051	1.168	0.24	4.1	6.99
NB-7	1.1	16.5	14.7	1.12	0.203	1.016	0.96	4.0	12.22
NB-11	1.1	17.8	14.7	1.22	0.203	1.016	0.96	4.8	13.19
NB-22	1.1	17.6	14.7	1.19	0.203	1.016	0.96	5.2	10.16
NB-19	1.1	17.5	14.7	1.19	0.356	0.864	1.68	4.3	9.69
NB-27	1.1	17.2	14.6	1.17	0.356	0.864	1.68	4.3	8.61
NB-36	1.1	15.5	14.7	1.05	0.356	0.864	1.68	5.2	10.71
NB-2	2.0	29.0	14.5	2.02	0.051	1.168	0.24	5.1	3.30
NB-5	2.0	29.1	14.7	1.95	0.051	1.168	0.24	5.2	2.21
NB-25	2.0	29.1	14.7	1.98	0.051	1.168	0.24	4.5	1.59
NB-20	2.0	29.7	14.9	2.00	0.203	1.016	0.96	4.6	3.96
NB-29	2.0	28.9	14.6	1.99	0.203	1.016	0.96	4.6	3.53
NB-31	2.0	27.5	14.6	1.87	0.203	1.016	0.96	4.1	4.15
NB-4	2.0	28.7	14.5	2.00	0.356	0.864	1.68	4.8	7.71
NB-14	2.0	27.9	14.7	1.88	0.356	0.864	1.68	4.9	5.62
NB-21	2.0	22.7	14.4	1.58	0.356	0.864	1.68	6.2	9.40
NB-6	3.0	43.0	14.4	3.01	0.051	1.168	0.24	4.8	0.29
NB-9	3.0	42.8	14.5	2.98	0.051	1.168	0.24	5.6	0.40
NB-12	3.0	42.2	14.6	2.91	0.051	1.168	0.24	4.8	0.88
NB-28	3.0	43.4	14.5	3.00	0.203	1.016	0.96	4.3	1.49
NB-32	3.0	42.6	14.4	2.99	0.203	1.016	0.96	4.3	1.90
NB-33	3.0	42.8	14.5	2.97	0.203	1.016	0.96	4.6	2.41
NB-16	3.0	41.8	14.6	2.87	0.356	0.864	1.68	4.0	2.49
NB-26	3.0	41.9	14.6	2.89	0.356	0.864	1.68	4.8	2.19
NB-35	3.0	43.6	14.6	3.00	0.356	0.864	1.68	4.8	2.62
NB-3	4.0	56.0	14.5	3.88	0.051	1.168	0.24	4.7	0.10
NB-13	4.0	55.8	14.6	3.81	0.051	1.168	0.24	4.7	0.11
NB-23	4.0	54.2	14.6	3.75	0.051	1.168	0.24	5.1	0.09
NB-8	4.0	57.4	14.5	4.02	0.203	1.016	0.96	4.8	1.05
NB-10	4.0	57.0	14.4	4.01	0.203	1.016	0.96	4.4	1.09
NB-30	4.0	56.3	14.6	3.90	0.203	1.016	0.96	4.2	1.45
NB-17	4.0	55.1	14.7	3.76	0.356	0.864	1.68	5.2	1.84
NB-24	4.0	53.6	14.6	3.70	0.356	0.864	1.68	4.9	1.81
NB-34	4.0	56.2	14.8	3.83	0.356	0.864	1.68	4.6	1.74

or

$$\Pi_2 * \Pi_1 = c \ln(\Pi_4) + d, \tag{3}$$

as shown in Figures 1 and 2.

Determination of parameters a, b, c, d in Equations (2) and (3) by regression of the data then allows these equations to be solved for the ARD concentration C in units of mg m^{-3} for any arbitrary dust generation rate R . In this manner, the effect of each variable Q_B, Q_C, H_S, A_S, A_L on the ARD, taken independently of the other variables, can be determined.

Although the “true” functional relationship between the Q parameters is not known, the logarithmic functional form of Equations (2) and (3) was chosen based on several considerations. First, $\Pi_2 * \Pi_1$ can reasonably be deduced to be a strictly decreasing monotonic function of Π_3 and Π_4 . Second, since $A_S > 0, H_S > 0$, and A_L has an upper limit defined by the condition of the absence of a shroud, both Π_3 and Π_4 must possess lower limits $\Pi_{3LL} > 0$ and $\Pi_{4LL} > 0$. Third, the logarithmic form can provide a more uniform rate of change of the dependent variable than a power function, and its use is not without precedence in aerosol science [10].

4. Results

Table 1 summarises the test parameters and results, categorised by Q_C/Q_B and A_L , for thirty-six tests. Figures 1(a) to (d) and 2(a) to (d) summarise the functional relationships

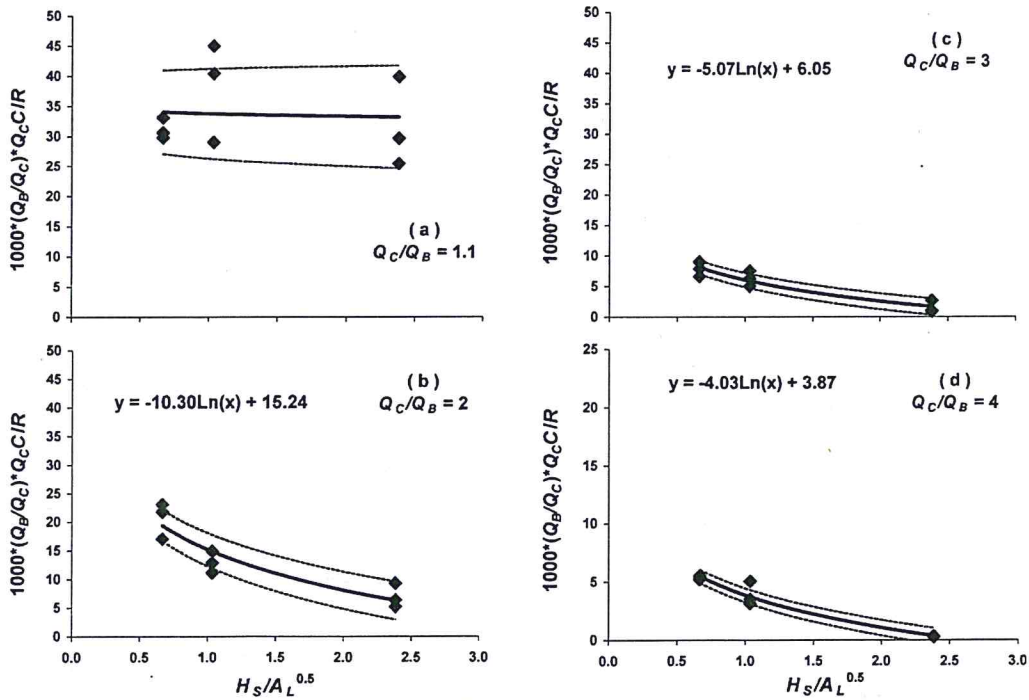


Figure 1. ARD concentration Π parameter as a function of the deck height to shroud leakage area ratio with 95% confidence bands.

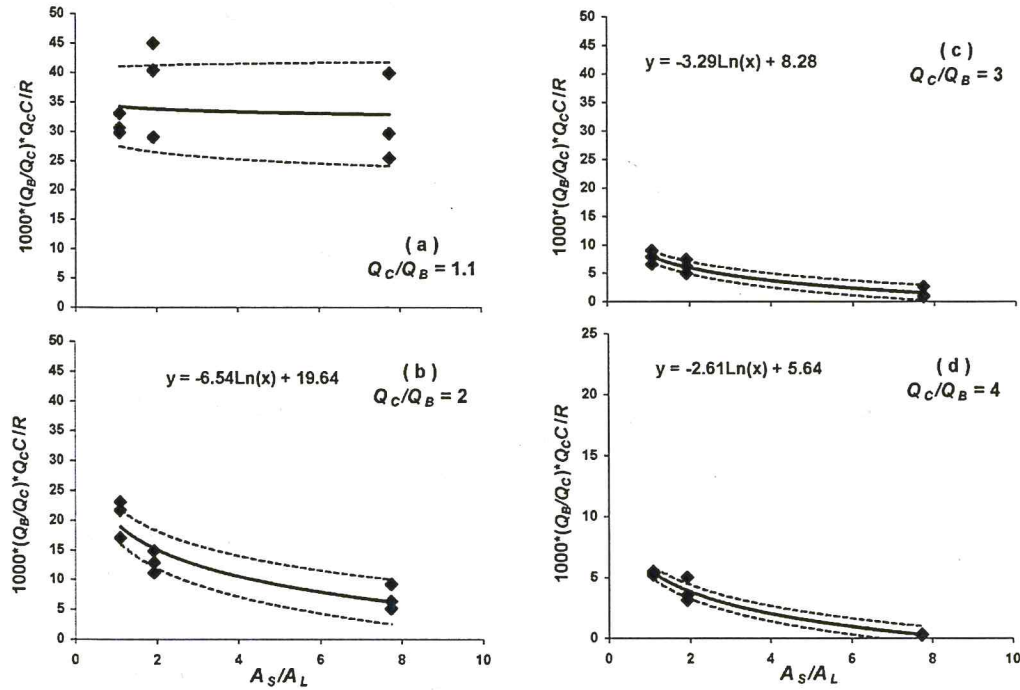


Figure 2. ARD concentration Π parameter as a function of the deck area to shroud leakage area (ratio) with 95% confidence bands.

between the dependent parameter $\Pi_2 \cdot \Pi_1$ and the independent parameters $\Pi_3 = H_S/A_L^{0.5}$ and $\Pi_4 = A_S/A_L$, respectively, and for the four ratios of Q_C/Q_B . The non-linear regressions were generally efficient with R^2 values ranging from 0.80 to 0.95 and the dashed lines are the regression 95% confidence bands. It is observed that for any values of parameters and an arbitrary material feed or generation rate R , it is possible to predict the ARD concentration. Table 2 summarises the solution for the ARD concentrations $C1$, $C2$, $C3$ and $C4$ for the parameter values tested. The values of $Q_C = 15, 30, 40$ and $60 \text{ m}^3 \text{ min}^{-1}$ approximate the values of Q_C experimentally tested in Table 1. In general, the function inversions for Π_3 and Π_4 at $Q_C/Q_B = 2$ are shown in Figures 3 and 4 for the four values of Q_C . The y-axes of Figures 3 and 4 intersect the x-axes at the value at which the independent variable is a minimum. This corresponds to the maximum value of A_L , which represents no deck shroud.

5. Discussion

5.1. Change of model for $Q_C/Q_B = 1.1$

It has been previously reported [6] that, given the operational parameters of this work, extrapolation of the curves in Figures 3 and 4 to the minimum values of the Π parameters would result in ARD values between 25 and 30 mg m^{-3} . Moreover, extrapolating the previously reported data for values of $Q_C/Q_B < 2$ would indicate similar decreases in ARD for increases in the Π parameters. However, it is seen from Figures 1 and 2 that this is not necessarily the case. Figures 1(a) and 2(a) clearly

Table 2. Respirable dust concentrations predicted by dimensional analysis, $R = 6365 \text{ mg min}^{-1}$.

Q_C/Q_B Target	A_S/A_L	A_S/A_L Regression coefficient	A_S/A_L Regression constant	Q_{C1} ($\text{m}^3 \text{ min}^{-1}$)	Q_{C2} ($\text{m}^3 \text{ min}^{-1}$)	Q_{C3} ($\text{m}^3 \text{ min}^{-1}$)	Q_{C4} ($\text{m}^3 \text{ min}^{-1}$)	C1 (mg m^{-3})	C2 (mg m^{-3})	C3 (mg m^{-3})	C4 (mg m^{-3})
1.1	1.11	-0.68	34.29	15	30	40	60	15.97	7.99	5.99	3.99
1.1	1.94	-0.68	34.29	15	30	40	60	15.79	7.90	5.92	3.95
1.1	7.74	-0.68	34.29	15	30	40	60	15.35	7.68	5.76	3.84
2.0	1.11	-6.54	19.64	15	30	40	60	16.11	8.05	6.04	4.03
2.0	1.94	-6.54	19.64	15	30	40	60	13.00	6.50	4.88	3.25
2.0	7.74	-6.54	19.64	15	30	40	60	5.31	2.66	1.99	1.33
3.0	1.11	-3.29	8.28	15	30	40	60	10.12	5.06	3.80	2.53
3.0	1.94	-3.29	8.28	15	30	40	60	7.78	3.89	2.92	1.94
3.0	7.74	-3.29	8.28	15	30	40	60	1.97	0.99	0.74	0.49
4.0	1.11	-2.61	5.64	15	30	40	60	9.12	4.56	3.42	2.28
4.0	1.94	-2.61	5.64	15	30	40	60	6.65	3.32	2.49	1.66
4.0	7.74	-2.61	5.64	15	30	40	60	0.51	0.25	0.19	0.13
		$H_S/A_L^{0.5}$ Regression coefficient	$H_S/A_L^{0.5}$ Regression constant								
1.1	0.67	-0.67	33.76	15	30	40	60	15.88	7.94	5.96	3.97
1.1	1.04	-0.67	33.76	15	30	40	60	15.75	7.87	5.90	3.94
1.1	2.39	-0.67	33.76	15	30	40	60	15.49	7.74	5.81	3.87
2.0	0.67	-10.3	15.24	15	30	40	60	16.48	8.24	6.18	4.12
2.0	1.04	-10.3	15.24	15	30	40	60	12.62	6.31	4.73	3.15
2.0	2.39	-10.3	15.24	15	30	40	60	5.34	2.67	2.00	1.33
3.0	0.67	-5.07	6.05	15	30	40	60	10.32	5.16	3.87	2.58
3.0	1.04	-5.07	6.05	15	30	40	60	7.47	3.73	2.80	1.87
3.0	2.39	-5.07	6.05	15	30	40	60	2.09	1.05	0.78	0.52
4.0	0.67	-4.03	3.87	15	30	40	60	9.35	4.67	3.50	2.34
4.0	1.04	-4.03	3.87	15	30	40	60	6.32	3.16	2.37	1.58
4.0	2.39	-4.03	3.87	15	30	40	60	0.62	0.31	0.23	0.16

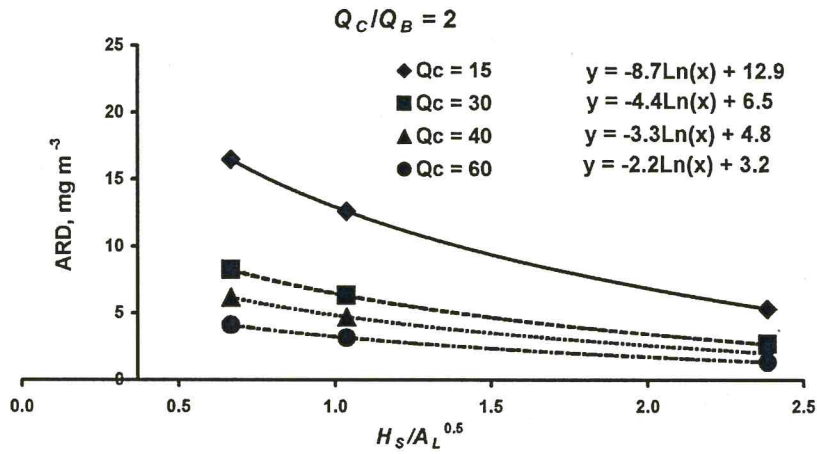


Figure 3. Predicted ARD concentration as a function of the deck height to shroud leakage area ratio for $Q_C/Q_B = 2$ and four values of Q_C ($\text{m}^3 \text{min}^{-1}$).

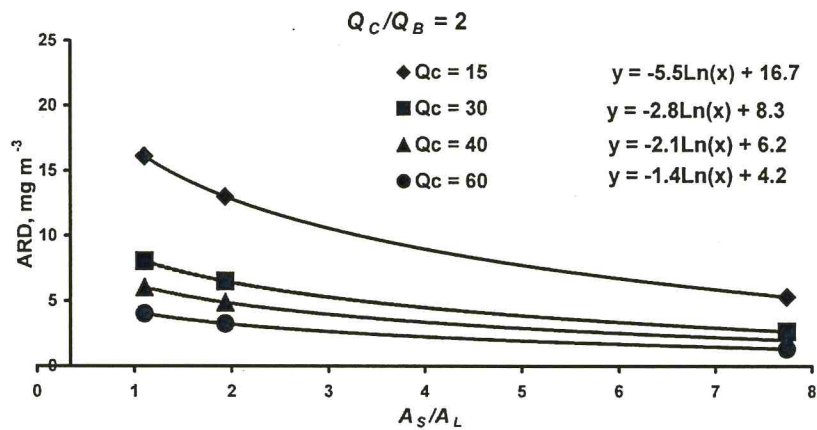


Figure 4. Predicted ARD concentration as a function of the deck area to shroud leakage area ratio for $Q_C/Q_B = 2$ and four values of Q_C ($\text{m}^3 \text{min}^{-1}$).

indicate that $Q_C/Q_B = 1.1$ would require reducing shroud leakage by amounts greater than achieved in this work. Doing so would require a near-perfect shroud seal or, alternatively, near zero leakage.

5.2. Practical usage of the model

The practical usefulness of any model representation is only achieved if it can be readily applied by the mine operator or engineer. Although this topic has been previously presented [6], it is presented again here because of its importance in enabling the mine operator or engineer to protect the health of surface miners by reducing dust emissions. Figures 3 and 4 present such a representation. By measuring a few basic parameters and using the equations presented in the figures, there are two methods of estimating the

relative severity of a drill's dust emissions as well as how much of a relative reduction can be obtained by changing any given parameter. Using Figure 4 for example, the parameters that must be measured or estimated are (1) the drill deck shroud area A_S , (2) an approximate amount of shroud leakage area A_L or a range for the leakage area, and (3) the bailing air flow rate, Q_B . Q_B is usually known from the drill manufacturer. It should be noted that Q_C is perhaps the more difficult parameter to measure and that dust collector specifications should not be used since collector air flow specifications are made under ideal conditions with unloaded filters. However, it will be observed that all four curves for differing Q_C follow the same trend and, as a result, it is not mandatory to know this value. The calculated value of ARD is not important because this is a relative value and the important consideration is where on the curve the drill operates. Therefore, as a first approximation, all that must be known is the ratio A_S/A_L . If a more precise estimate is needed, then it is necessary to measure Q_C . Making this measurement will allow applying the correct equation in Figure 4 as well as determining Q_C/Q_B . Knowing this ratio will allow the user to estimate on a more absolute basis the magnitude of the drill dust emissions using Figures 1 or 2.

These determinations will indicate the long-term average improvement that can be expected from either increasing the collector air flow (installing a larger collector, for example) or reducing the amount of shroud leakage.

6. Conclusions

A semi-empirical mathematical model has been developed and expanded to describe ARD generation on surface coal mine drills. Geometric parameters included are drill deck height and cross-sectional area, shroud leakage associated with the deck shroud, and the operational parameters of bailing airflow and dust collector airflow. The relationships appear to be described by logarithmic functions and yield predictive ARD values which fall in the range measured on operating drills for collector/bailing air flow ratios greater than 2. However, at values of collector/bailing air flow ratios of approximately 1.1 the amount of ARD shows minimal response, if any, to drill deck shroud improvements that do not result in near-perfect seals. Application of these results should provide mine operators with sufficient information to determine (1) the relative magnitude of their dust emissions, (2) where they should focus their efforts to reduce ARD emissions, and (3) the improvement they could reasonably expect to achieve. Given that exposures of surface coal mine rock drillers to respirable crystalline silica are of particular concern, significant reductions of airborne silica dust during drilling may be estimated and achieved through use of the analysis presented.

7. Disclaimer

The findings and conclusions in this report are those of the authors and do not necessarily represent the views of the National Institute for Occupational Safety and Health (NIOSH). Mention of any company or product does not constitute endorsement by NIOSH.

References

- [1] National Institute for Occupational Safety and Health (NIOSH), *Request for assistance in preventing silicosis and deaths in rock drillers*, NIOSH ALERT, DHHS (NIOSH), Publication No. 92-107, 1992, p. 15.

- [2] P.A. Tyson, J.L. Stauffer, E.A. Mauger, et al. *Silicosis screening in surface coal miners – Pennsylvania, 1996–1997*, MMWR 49 (2000), pp. 612–615.
- [3] U.S. Code of Federal Regulations, Title 30 – Mineral Resources; Chapter I – Mine Safety and Health Administration, Dep. Labor; Subchapter O, Coal Mine Safety and Health, Part 70-Mandatory Health Standards – Underground Coal Mines, Subpart B, Section 70.101; and Part 71-Mandatory Health Standards – Surface Coal Mines and Surface Work Areas of Underground Coal Mines, Subpart B, Section 71.101. U.S. Gov. Printing Office, Office of Federal Regulations, 2001.
- [4] T.F. Tomb, A.J. Gero, and J. Kogut, *Analysis of quartz exposure data obtained from underground and surface coal mining operations*, Appl. Occup. Environ. Hyg. 10 (1995), pp. 1019–1026.
- [5] S.D. Maksimovic, and S.J. Page, *Quartz dust sources during overburden drilling at surface coal mines*, US Bureau Mines Information Circular IC 9056 (1985).
- [6] S.J. Page, and J.A. Organiscak, *Semi-empirical model for predicting surface coal mine drill respirable dust emissions*, Int. J. Surface Min., Recl. And Env. 1 (2004), pp. 42–59.
- [7] E. Buckingham, *Model experiments and the form of empirical equations*, Trans. ASME 37 (1915), pp. 263–296.
- [8] S.J. Page and J.A. Organiscak, *New shroud design controls silica dust from surface mine and construction blast hole drills*, Cincinnati, OH: U.S. Department of Health & Human Services, Public Health Service, CDC\NIOSH Hazard Control No. 27, 1998.
- [9] S.J. Page and J.A. Organiscak, *Taming the dust devil – An evaluation of improved dust controls for surface coal mine drills using rotoclone collectors*, Eng. Min. J. 196 (1995), pp. 30–31.
- [10] W.C. Hinds, *Aerosol Technology: Properties, Behaviour, and Measurement of Airborne Particles*, Wiley, New York, 1982, p. 84.